Cercetări Agronomice în Moldova
Vol. XLVII , No. 4 (160) / 2014

MODELING DRYING CHARACTERISTICS OF TEREBINTH FRUIT UNDER INFRARED FLUIDIZED BED CONDITION

M. KAVEH[1], R. AMIRI CHAYJAN[1]*

*E-mail: amirireza@basu.ac.ir

Received January 3, 2014

ABSTRACT. Advantages of infrared fluid bed drying include high heat and mass transfer coefficients, short process time, high quality and low energy consumption. Since heat and mass transfer and quality changes during drying of terebinth fruit with infrared fluid bed method is not described in the literature. Goals of this research were study the effects of different infrared drying conditions on the drying kinetic and physical parameters of terebinth fruit. To predict moisture during drying process, five mathematical models were used. Experiments were conducted at different levels of hot air velocity (0.93, 1.76 and 2.6 m/s), temperature (40, 55, and 70°C) and infrared radiation power (500, 1000 and 1500 W). Results showed that Demir *et al.* model had the best performance for predicting of moisture ratio. Effective moisture diffusivity for terebinth samples (6.2×10^{-11} to 7.3×10^{-10} m^2/s) was achieved. Activation energy of the samples (44.4 to 59.13 kJ/mol) was computed. Maximum rupture force (118.4 N) was calculated at air velocity of 2.6 m/s, infrared power of 1500 W and air temperature of 70°C. The results proved that in addition to short process time, monitoring of terebinth fruit characteristics such as mechanical properties during drying process can be achieved.

Key words: Terebinth; Drying; Thin layer; Activation energy; Rupture force.

INTRODUCTION

Terebinth (*Pistacia atlantica* L.) is an ancient and long life tree with about 5 m height. May and June is the ripening time of terebinth fruit. Terebinth fruit is small and spherical-like with dark green color. Flesh of terebinth is similar to pistachio, but much smaller than (Kaveh and Amiri Chayjan, 2014). Terebinth fruit is used in buttermilk process and animal oils and is also used to make pickles. The harvested terebinth fruit has too much moisture (about 1.16 % d.b.). This causes fast spoilage of the fruit.

Drying is defined as moisture reduction from the products. It is a most important process for preserving of agricultural and food products

[1] Department of Biosystems Engineering, Faculty of Agriculture, Bu-Ali Sina University, Hamedan, Iran

since it has a significant effect on the quality of the products. The major objective in drying of food and agricultural products is to safe storage of them over an extended period (Doymaz, 2004a).

Infrared (IR) drying has emerged as one of the potential additions to the common drying method because of its intrinsic benefits such as simplicity of the required equipment, easy accommodation of IR drying with conductive, convective and microwave methods, greater heat transfer rate, significant energy saving and fast transient response (Boudhrioua *et al*., 2009; Basman and Yalcin, 2011). Infrared drying involves the exposure of the humid material to the wavelength range of 0.8 - 1000 μm of electromagnetic radiation (Das *et al*., 2009). Many researchers studied IR drying as a potential method to obtain high quality dried fruits, vegetables and grains (Ruiz Celma *et al*., 2009a; Khir *et al*., 2011). Many studies have been carried out about increasing heating efficiency and producing high quality of dried foodstuffs (Wang and Sheng, 2006; Zhu *et al*., 2010; Dondee *et al*., 2011).

When infrared radiation is used to dry moist materials, the radiation impinges the exposed material, penetrates it and the radiation energy is converted into heat (Pan *et al*., 2008).

Several empirical models for drying kinetics in falling rate period are presented in literature. These models vary widely in nature. Many researchers have successfully used these models to predict drying kinetics of several food and agricultural products (Togrul and Pehlivan, 2004; Bozkir, 2006; Shi *et al*., 2008; Amiri Chayjan *et al*., 2011).

The mathematical modeling of mass transfer is a very useful approach in studying the intrinsic kinetics of a drying process. Empirical models can predict a direct relationship between moisture ratio (MR) and drying time. Various mathematical models were developed in order to describe the IR drying characteristic for different agricultural products (Shi *et al*., 2008; Duc *et al*., 2011; Doymaz and Ismail, 2011; Ponkham *et al*., 2011).

The mechanical properties of food and agricultural materials are important issues to be considered during the design, development and effective utilization of the equipment used for processing, packaging, transportation and storage of the products (Amiri Chayjan and Kaveh, 2013). Moreover, mechanical properties such as the rupture force and the energy used for rupturing nut and kernel are taken into account when designing nut shelling and kernel grinding machinery (Altuntas *et al*., 2010; Gharibzahedi *et al*., 2010). Many researchers evaluated the mechanical properties of different agricultural products, including faba bean (Altuntas and Yildiz, 2007), shea kernel (Manuwa and Muhammad, 2011) and walnut (Gharibzahedi *et al*., 2012).

The main objectives of this study were to present a mathematical model

suitable for predicting the drying kinetic of terebinth under infrared fluidized bed drying conditions and for determining the effective moisture diffusivity, activation energy, rupture force and energy of terebinth fruit during thin layer infrared fluidized bed drying process and their dependence on factors such as input air temperature, air velocity and IR radiation.

MATERIALS AND METHODS

Experimental setup. Fresh terebinth fruits were supplied from Sardasht forests, west Azerbaijan, Iran. To carry out the drying tests was kept at refrigerator temperature 4°C. Initial moisture content of terebinth fruit was determined by oven method at a temperature of 105±1°C for 24 hours (Doymaz, 2005). The initial moisture content of the fruit was 1.16 (d.b). For the beginning the pressure drop over a bed of terebinth fruits was evaluated for different air flow velocities. Fan speed was gradually increased using an inverter (Vincker VSD2, Taiwan) and air velocity and pressure drop were recorded using a multifunction measurement device (Standard ST-8897, China); the device contains a vane type digital anemometer with ±0.1 m/s accuracy and a differential manometer with ±0.1 Pa accuracy.

The drying experiments were conducted using a laboratory infrared-fluidized bed dryer (*Fig. 1*). Three experimental points were selected on the fluidization curve (*Fig. 2*): fix bed at 0.93 m/s (point A), semi fluidized bed at 1.76 m/s (point B) and fluidized bed at 2.6 m/s (point C). The experiments were performed at three air temperatures (40, 55, and 70°C); three different infrared powers (500, 1000 and 1500 W) were used in the experiments.

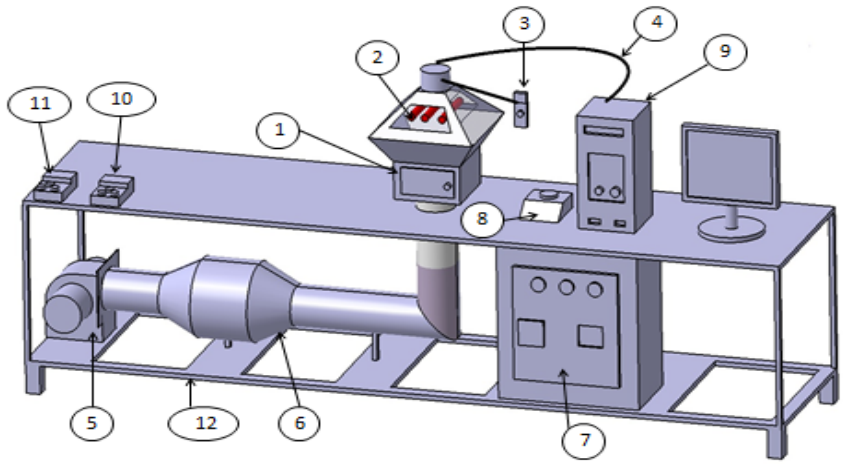

Figure 1 - Schematic diagram of laboratory scale infrared-fluidized bed dryer: (1) drying chamber (2) infrared lamp, (3) thermocouple, (4) air velocity sensor, (5) fan and electrical motor, (6) electrical heater, (7) inverter and thermostat, (8) precision balance, (9) computer, (10) thermometer, (11) psychrometer and (12) chassis

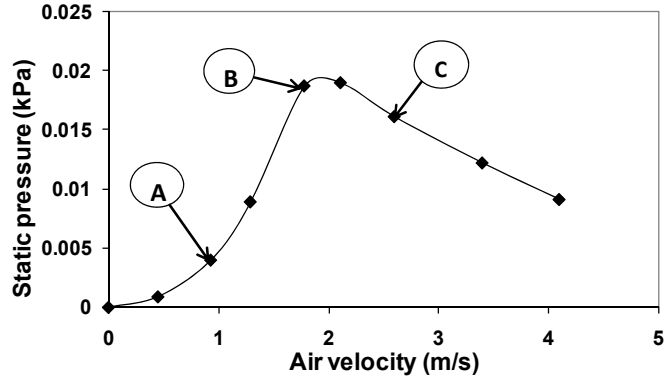

Figure 2 - Fluidization curve of terebinth seeds and selected point for modeling: A- fix bed (0.93 m/s), B- semi fluid bed (1.76 m/s) and C- fluid bed (2.6 m/s)

The terebinth bed contained aprox. 30 g of fruit, uniformly spread over a perforated plate which was placed inside the dryer. The drying time was considered as the time required for reducing the moisture content of the product to 0.2 (d.b.). The drying experiments were conducted in three replicates.

Kinetic modeling. The moisture ratio (MR) of terebinth fruit during the thin layer infrared drying was calculated as follows:

$$MR = \frac{M_a - M_e}{M_b - M_e} \quad (1),$$

where MR is the moisture ratio, M_a is the moisture content at time t (% d.b.), M_b and M_e are the initial and equilibrium moisture contents, respectively (% d.b.).

Empirical modeling was used as an alternative method to analyze the thin layer drying process. Five commonly models which used in thin layer drying of terebinth fruit are presented in *Table 1*. In order to select a suitable mathematical model for describing the drying process of terebinth fruit, thin layer drying equations were fitted to drying curves.

Table 1 - Thin layer drying models used in modeling of terebinth fruit

Models	Equation	Refrens
Demir *et al*.	$MR=a \exp(-kt)^n+b$	Demir *et al*. (2007)
Midilli *et al*.	$MR=a \exp(-kt^n)+bt$	Ruiz Celma *et al.* (2009b)
Page	$MR=\exp(-kt^n)$	Arumuganathan *et al.* (2009)
Logestic	$MR=a/(1+b \exp(kt))$	Amiri Chayjan and Kaveh (2013)
Two-term	$MR=a \exp(k_0t)+b \exp(-k_1t)$	Sharma *et al*. (2005)

a, b, c, k, k_0,k_1 and n are drying constants.

During drying of terebinth fruit in the infrared dryer, M_e values were relatively small compared to M_a and M_b. So the Eq. (1) was simplified as follow (Shi *et al*., 2008):

$$MR = \frac{M_a}{M_b} \quad (2)$$

Five thin layer models (*Table 1*) were used in order to fit to the experimental drying curves. The constants involved in the respective models were obtained using nonlinear regression of Curve Expert software (Vers. 1.4). The goodness of fit for all the models was evaluated using three indices: Pearson coefficient (R^2), chi-square (χ^2) and root mean squared error (RMSE):

$$R^2 = 1 - \frac{\sum_{i=1}^{N}[MR_{exp,i} - MR_{pre,i}]^2}{\sum_{k=1}^{N}\left[\frac{\sum_{k=1}^{n} MR_{pre,i}}{N} - MR_{pre,i}\right]^2} \quad (3)$$

$$\chi^2 = \frac{\sum_{i=1}^{N}\left(MR_{exp,i} - MR_{pre,i}\right)^2}{N - z} \quad (4)$$

$$RMSE = \left[\frac{1}{N}\sum_{i=1}^{N}(MR_{pre,i} - MR_{exp,i})^2\right]^{\frac{1}{2}} \quad (5),$$

where $MR_{exp,i}$ is the experimental moisture ratio of i^{th} data, $MR_{pre,i}$ is the predicted moisture ratio of i^{th} data, N is the number of observations and z is the number of drying constants.

The best model was considered to be the one with the highest R^2 value and the lowest χ^2 and RMSE values (Amiri Chayjan and Kaveh, 2013).

Effective moisture diffusivity. Drying of agricultural and food products generally occurs under falling rate period. In the other words, constant rate in more agricultural products is very short. Diffusion is one of the most effective physical phenomena to govern the moisture movement (Das *et al*., 2009). It is recommended that dehydration process for porous materials, during the the falling rate period of drying, should be estimated using Fick's second law of diffusion (Abbasi Souraki and Mowla, 2008). The effective moisture diffusivity (D_{eff}), at any suggested moisture content level can be calculated using technique of slope method (Das *et al*., 2009).

The second diffusion law of Fick, considering the spherical geometry, was applied in this study. The assumptions of this method were: moisture transfer occurs through diffusion; the temperature the diffusion coefficients were assumed to be constant (Niamnuy *et al*., 2012):

$$MR = \frac{M_a - M_e}{M_b - M_e} = \frac{6}{\pi^2}\sum_{n=1}^{\infty}\frac{1}{n^2}\exp\left(\frac{-D_{eff}n^2\pi^2 t}{r^2}\right) \quad (6),$$

where n = 1, 2, 3, ... is the number of terms taken into consideration; t is the drying time, (s); D_{eff} is the effective moisture diffusivity (m^2/s); r is the radius of kernel (m).

For long drying periods only the first term of series form Eq. (6) can be considered, without much affecting on the prediction accuracy (Caglar *et al*., 2009):

$$MR = \left(\frac{6}{\pi^2}\right)\exp\left(-\frac{\pi^2 D_{eff} t}{r^2}\right) \quad (7)$$

Then:

$$\ln(MR) = \ln\left(\frac{M_a - M_e}{M_b - M_e}\right) = \ln\left(\frac{6}{\pi^2}\right) - \left(\frac{D_{eff}\pi^2 t}{r^2}\right) \quad (8)$$

The slope (K_1) is computed by plotting ln(MR) versus time, according to Eq. (9) (Babalis and Belessiotis, 2004):

$$K_1 = \left(\frac{D_{eff}\pi^2}{r^2}\right) \quad (9)$$

Activation energy. An Arrhenius-type equation was used to calculate the activation energy (Khir *et al*., 2011; Niamnuy *et al*., 2012):

$$D_{eff} = D_0 \exp\left(\frac{E_a}{R_g T_a}\right) \quad (10)$$

$$\ln(D_{eff}) = \ln(D_0) - \left(\frac{E_a}{R_g}.\frac{1}{T_a}\right) \quad (11),$$

where E_a is the activation energy (kJ/mol); R_g is the universal gas constant (8.3143 kJ/(mol K)); T_a is the absolute air temperature (K); D_0 is the pre-exponential factor of the Arrhenius equation (m^2/s).

Plotting $\ln(D_{eff})$ against $\frac{1}{T_a}$, using Eq. (11), leads to a straight line, with the slope K_2:

$$K_2 = \frac{E_a}{R_g} \quad (12)$$

A linear regression analysis was used to fit the equations to the experimental data and the Person coefficient (R^2) was calculated.

Rupture force and energy. The mechanical properties of terebinth fruit (rupture force and energy) are useful in designing and optimizing of the fruit shelling and kernel grinding machinery. These properties are affected by numerous factors including moisture content, drying method and temperature. Minimum required force for fruit shelling and kernel grinding is specified by the rupture force (Altuntas *et al*., 2010).

A materials testing machine (Zwick/Roell, Germany) was used during the experiments; the equipment allowed the evaluation of the mechanical characteristics of terebinth fruits during compression tests. The apparatus was equipped with a 5 kN load cell. The precision of the measurements was ±0.001 N for force and 0.0001 mm for deformation. The terebinth fruit was placed on the plate moving with the speed of 5 mm/min and pressed towards the fixed plate, equipped with the load, cell until rupture occurred.

The grain fracture on the force-deformation curve is a point that after it the deformation rate is increases even with reduces in the applied force and the body is broken. This point is defined as the rupture point. In the hard and soft materials, an intrinsic transformation occurs after rupture. Thus, in different studies on the force-deformation curve, the maximum force was obtained in fruit failure. Experimental data were transferred to Excel software in order to calculate the area under the force-deformation curve, using the trapezoidal method; the estimated area is equal to the rupture energy for the terebinth fruit.

RESULTS AND DISCUSSION

Mathematical modeling of drying kinetics. The drying kinetic of terebinth samples for all bed conditions and temperatures are presented in *Fig. 3*. The average final moisture content of terebinth samples was about 0.19 (d.b.). According to the results, drying air temperature and infrared radiation had important role in drying time. When air temperature and IR radiation was increased, the drying time was decreased.

The average moisture ratio of dried terebinth fruits at different temperatures was verified using five mathematical models to find out their

suitability to describe the drying behavior. R^2, χ^2 and RMSE of models are presented in *Table 2*. The best model should have the highest R^2 value and the lowest χ^2 and RMSE values. The R^2 values for Demir *et al*., Page, Midilli *et al*., Two-term and Logestic models were higherr than 0.99 (*Table 2)*; the Demir *et al.* model led to higher R^2 values, for all the drying temperatures considered, while the values for χ^2 and RMSE were the lowest. As a result it was decided to use the Demir *et al*. model in order to describe the infrared drying process of terebinth fruits. The coefficients involbed in the Demir *et al.* model, for all temperatures and bed conditions, are presented in *Table 3*.

Effective moisture diffusivity. Moisture ratio variations [ln(MR) values against drying time in hours] of terebinth fruits for each air velocity, temperature and IR power are presented in *Figs. 3 and 4.* The charts show that the drying process of terebinth fruit occurred in falling rate period; the slope of the drying curves increased with the increasing input temperature.

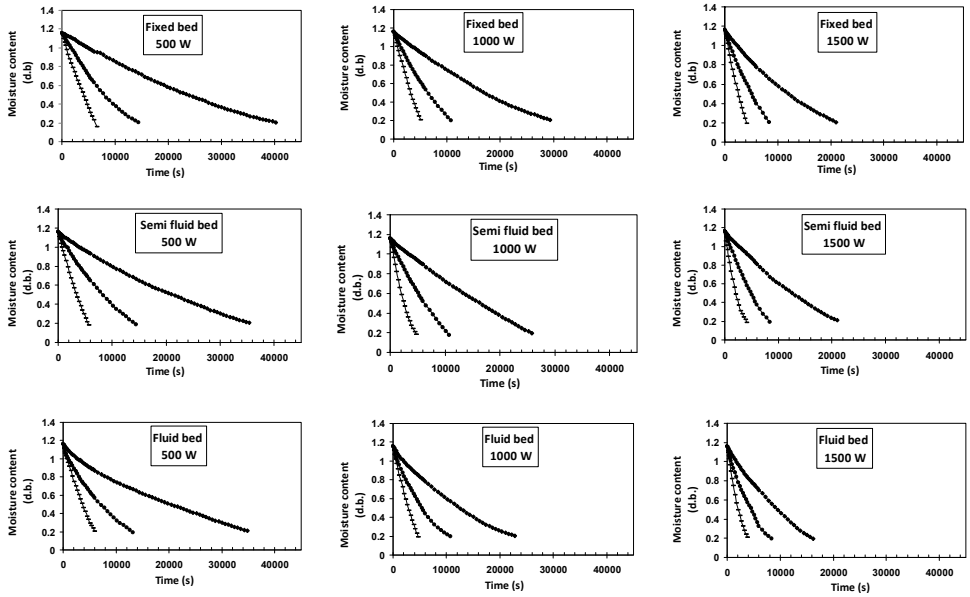

Figure 3 - Moisture content variation of terebinth seed under infrared drying process (♦ 40 °C, ● 55 °C, —70 °C)

Table 2 - The statistical comparison for prediction of thin layer drying of terebinth seed

Model	Temperature (°C)- IR radiation (W)	R^2			χ^2			RMSE		
		0.93 m/s	1.76 m/s	2.6 m/s	0.93 m/s	1.76 m/s	2.6 m/s	0.93 m/s	1.76 m/s	2.6 m/s
Demir *et al.*	40-500	0.9999	0.9998	0.9976	2.6E-4	5.8E-4	1.0E-2	0.0156	0.0234	0.0973
	55-500	0.9991	0.9998	0.9991	2.2E-3	3.7E-4	1.8E-3	0.0444	0.0183	0.0394
	70-500	0.9996	0.9997	0.9993	5.2E-4	3.2E-4	9.5E-4	0.0209	0.0161	0.0280
	40-1000	0.9995	0.9999	0.9994	1.7E-3	2.2E-4	2.0E-3	0.0397	0.0142	0.0433
	55-1000	0.9999	0.9999	0.9989	1.1E-4	9.1E-5	2.0E-3	0.0096	0.0089	0.0424
	70-1000	0.9997	0.9988	0.9998	3.8E-4	1.5E-3	1.4E-4	0.0175	0.0342	0.0105
	40-1500	0.9999	0.9995	0.9996	5.2E-5	1.6E-3	9.4E-4	0.0069	0.0382	0.0291
	55-1500	0.9996	0.9995	0.9982	3.9E-4	8.4E-4	2.9E-3	0.0183	0.0267	0.0504
	70-1500	0.9996	0.9982	0.9994	3.7E-4	2.2E-3	5.9E-4	0.0169	0.0409	0.0210
Midilli *et al.*	40-500	0.9949	0.9961	0.9970	2.5E-2	1.9E-2	1.2E-2	0.1559	0.1331	0.1098
	55-500	0.9999	0.9998	0.9996	1.6E-4	3.8E-4	6.3E-4	0.0121	0.0185	0.0237
	70-500	0.9998	0.9998	0.9993	2.6E-4	2.9E-4	9.7E-4	0.0148	0.0154	0.0284
	40-1000	0.9963	0.9999	0.9995	1.3E-2	2.1E-4	1.4E-3	0.1103	0.0139	0.0364
	55-1000	0.9999	0.9999	0.9988	7.6E-5	4.7E-5	2.1E-3	0.0081	0.0063	0.0433
	70-1000	0.9998	0.9999	0.9999	1.5E-4	8.5E-5	9.2E-5	0.0112	0.0082	0.0085
	40-1500	0.9999	0.9996	0.9997	5.2E-5	9.4E-4	5.6E-4	0.0069	0.0294	0.0224
	55-1500	0.9997	0.9997	0.9982	4.1E-4	4.0E-4	3.0E-3	0.0188	0.0184	0.0505
	70-1500	0.9998	0.9990	0.9999	1.3E-4	1.2E-3	1.1E-4	0.0102	0.0308	0.0092
Page	40-500	0.9984	0.9974	0.9950	8.7E-3	1.2E-2	2.1E-2	0.0920	0.1085	0.1416
	55-500	0.9998	0.9973	0.9963	4.2E-4	6.2E-3	7.5E-3	0.0199	0.0770	0.0842
	70-500	0.9936	0.9966	0.9956	1.0E-2	5.2E-3	6.8E-3	0.0974	0.0693	0.0786
	40-1000	0.9982	0.9957	0.9972	7.1E-3	1.5E-2	9.4E-3	0.0833	0.1218	0.0955
	55-1000	0.9982	0.9965	0.9974	3.4E-3	6.6E-3	4.9E-3	0.0563	0.0787	0.0677
	70-1000	0.9976	0.9999	0.9977	3.3E-3	8.9E-5	3.0E-3	0.0548	0.0089	0.0520
	40-1500	0.9990	0.9982	0.9964	3.0E-3	5.8E-3	9.1E-3	0.0540	0.0745	0.0933
	55-1500	0.9977	0.9981	0.9958	3.7E-3	3.2E-3	7.0E-3	0.0582	0.0543	0.0807
	70-1500	0.9981	0.9987	0.9998	2.2E-3	1.6E-3	1.4E-4	0.0446	0.0377	0.0112

Table 2 (continued)

Model	Temperature (°C)- IR radiation (W)	R^2			χ^2			RMSE		
		0.93 m/s	1.76 m/s	2.6 m/s	0.93 m/s	1.76 m/s	2.6 m/s	0.93 m/s	1.76 m/s	2.6 m/s
Logestic	40-500	0.9996	0.9991	0.9967	2.2E-3	4.2E-3	1.4E-2	0.0459	0.0634	0.1157
	55-500	0.9998	0.9992	0.9985	3.3E-4	1.8E-3	3.0E-3	0.0174	0.0409	0.0518
	70-500	0.9969	0.9990	0.9990	5.0E-3	1.5E-3	1.4E-3	0.0658	0.0356	0.0355
	40-1000	0.9997	0.9988	0.9990	9.7E-4	4.5E-3	3.3E-3	0.0303	0.0653	0.0556
	55-1000	0.9993	0.9988	0.9989	1.2E-3	2.2E-3	2.0E-3	0.0329	0.0450	0.0429
	70-1000	0.9995	0.9997	0.9993	6.4E-4	3.3E-4	9.1E-4	0.0234	0.0167	0.0276
	40-1500	0.9997	0.9994	0.9985	8.7E-4	1.8E-3	3.7E-3	0.0285	0.0407	0.0583
	55-1500	0.9990	0.9997	0.9977	1.6E-3	5.0E-4	3.7E-3	0.0379	0.0209	0.0575
	70-1500	0.9992	0.9990	0.9998	9.5E-4	1.2E-3	1.5E-4	0.0280	0.0315	0.0112
Two-term	40-500	0.9999	0.9999	0.9987	5.7E-4	1.2E-3	5.3E-3	0.0232	0.0346	0.0709
	55-500	0.9991	0.9998	0.9993	2.5E-3	7.4E-4	1.4E-3	0.0474	0.0257	0.0357
	70-500	0.9997	0.9997	0.9859	3.4E-4	3.8E-4	2.2E-2	0.0168	0.0176	0.1344
	40-1000	0.9995	0.9998	0.9993	2.6E-2	2.0E-2	2.0E-3	0.1575	0.1364	0.0435
	55-1000	0.9999	0.9999	0.9989	1.3E-4	6.7E-5	2.0E-3	0.0108	0.0076	0.0422
	70-1000	0.9996	0.9989	0.9998	3.9E-4	1.6E-3	1.4E-4	0.0176	0.0358	0.0107
	40-1500	0.9999	0.9994	0.9996	7.6E-5	1.8E-3	8.2E-4	0.0083	0.0404	0.0273
	55-1500	0.9997	0.9995	0.9982	4.4E-4	9.3E-4	3.0E-3	0.0194	0.0282	0.0506
	70-1500	0.9996	0.9983	0.9995	4.2E-4	2.0E-3	5.4E-4	0.0180	0.0395	0.0200

Table 3 - Coefficients of Demir *et al.* (2007) model for prediction of kinetic drying of terebinth seed

Bed condition	Coefficients	40°C-500W	55°C-500W	70°C-500W	40°C-1000W	55°C-1000W	70°C-1000W	40°C-1500W	55°C-1500W	70°C-1500W
Fix bed (0.93 m/s)	a	1.34	1.31	2.46	1.48	1.52	2.20	1.26	1.56	1.86
	k	0.297	0.512	0.483	0.318	0.515	0.580	0.424	0.571	0.722
	n	0.297	0.512	0.483	0.318	0.515	0.580	0.424	0.571	0.722
	b	-0.345	-0.297	-0.146	-0.480	-0.512	-0.119	-0.262	-0.554	-0.850
Semi fluid bed (1.76 m/s)	a	1.43	1.42	2.00	2.26	1.59	1.30	1.58	1.66	1.13
	k	0.292	0.476	0.590	0.252	0.500	0.923	0.358	0.557	1.11
	n	0.292	0.476	0.590	0.252	0.500	0.923	0.580	0.557	1.11
	b	-0.440	-0.433	1.004	1.270	-0.596	-0.280	-0.575	-0.651	-0.122
Fluid bed (2.6 m/s)	a	1.13	1.13	1.87	1.21	1.11	1.68	1.46	1.24	1.18
	k	0.342	0.577	0.591	0.421	0.673	0.723	0.430	0.692	1.08
	n	0.342	0.577	0.591	0.421	0.673	0.723	0.430	0.692	1.08
	b	-0.166	-0.163	-0.881	-0.227	-0.129	-0.675	-0.470	-0.254	-0.164

Table 4 - Activation energy values and related correlation coefficient for different bed conditions of terebinth seed

Air velocity (m/s)-Infrared (W)	0.93-500	0.93-1000	0.93-1500	1.76-500	1.76-1000	1.76-1500	2.6-500	2.6-1000	2.6-1500
Activation energy (Ea) (kJ/mol)	55.58	52	50.06	59.13	57.72	51.89	55.87	49.6	44.41
Coefficient of determination (R^2)	0.9968	0.9972	1	0.9951	0.9994	0.9998	0.9954	0.9983	0.9986

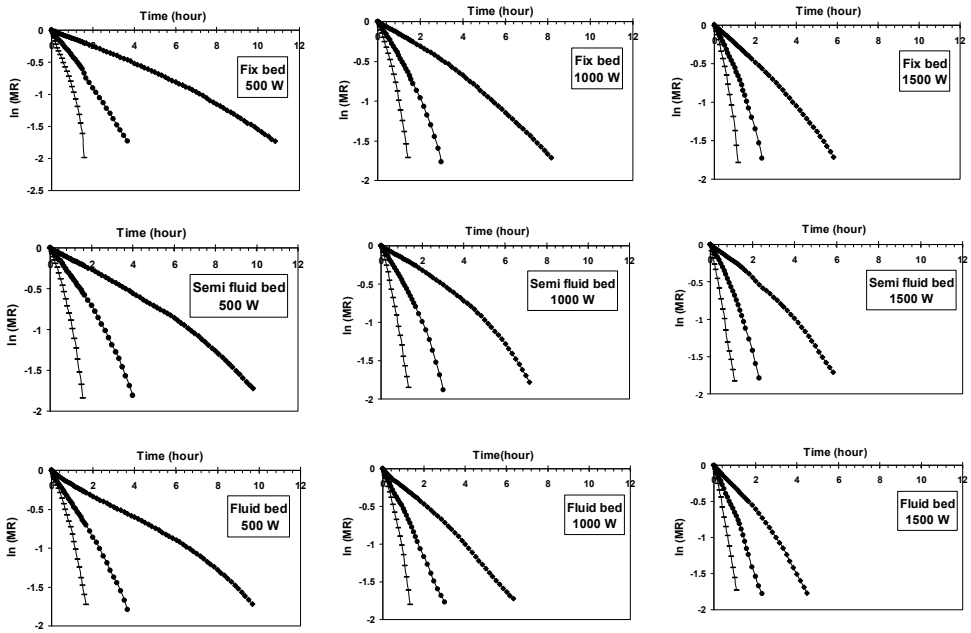

Figure 4 - $\ln(MR)$ **versus time (hour) for different bed conditions and drying air temperatures (♦ 40 °C, ● 55 °C and —70 °C)**

A direct relationship was found between IR radiation power and D_{eff}: increasing IR radiation power led to the increase of D_{eff}. The average effective moisture diffusivity (D_{eff}) was calculated by taking the arithmetic mean of the effective moisture diffusivities that were estimated at various levels of moisture contents during the drying period. The results concerning the effective moisture diffusivity are presented in (*Fig. 5*). The D_{eff} values obtained for terebinth fruit ranged from 6.11×10^{-11} to 7.3×10^{-10} m^2/s, which is within the generally reported range of 10^{-11} to 10^{-9} m^2/s for drying of food materials (Sacilik *et al.*, 2006): 0.2514×10^{-10} to 0.3233×10^{-10} m^2/s for onion slices (Pathare and Sharma, 2006), 11.013×10^{-9} to 26.050×10^{-9} m^2/s for grapes (Ruiz Celma *et al.*, 2009b), 4.87×10^{-11} to 1.29×10^{-9} m^2/s for corn (Amiri Chayjan *et al.*, 2011) and 8.21×10^{-10} to 2.61×10^{-9} m^2/s for castor oil fruits (Perea-Flores *et al.*, 2012). Results indicated that due to hard layer of terebinth shell, moisture elimination was conducted slowly compared to the mentioned crops. For the same conditions of air temperature and velocity, the registered D_{eff} values increased progressively as the power of the applied IR radiation was increased, reducing the drying time significantly. It was noticed that, for an air velocity of 2.6 m/s, the D_{eff} decreased at all air temperatures and

IR powers compared to similar drying conditions for air velocities of 0.93 and 1.76 m/s, a trend which contrary to convective drying. This is due to cooling of terebinth fruits at higher air velocity because the product temperature remained higher than surrounding air, resulting in negative temperature gradient.

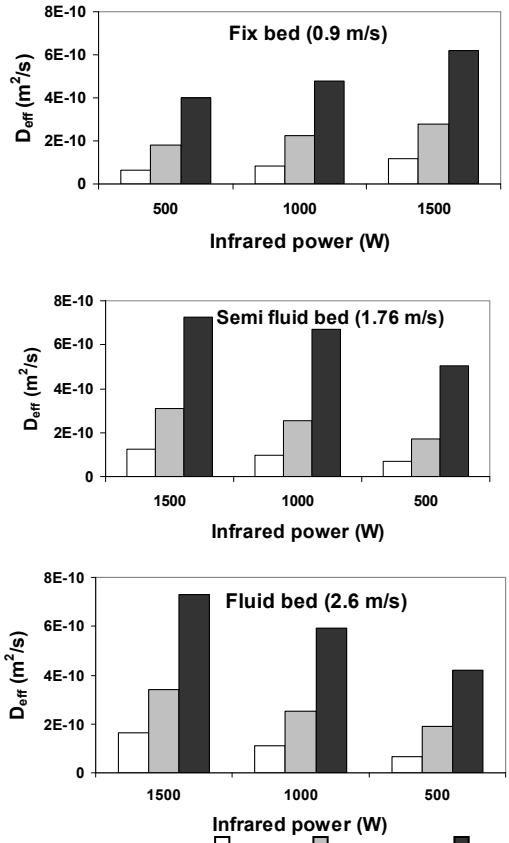

Figure 5 - D_{eff} versus air temperature (□ 40 °C, ▒ 55 °C and ■ 70 °C) and IR radiation (W/m^2) for drying terebinth seed

The relationship between D_{eff} and the independent variables is as follow:

where v is the air velocity (m/s), T_c is the air temperature (°C) and w is infrared power (W).

$$D_{eff} = 0.1334\times10^{-6}\,v + 0.2192\times10^{-11}\,T_c - 0.3217\times10^{-12}\,w - 0.1335\times10^{-6}\,vT_c + 0.2650\times10^{-11}\,T_c w + 0.8439\times10^{-14}\,vw \qquad R^2 = 0.9300 \quad (13),$$

Activation energy. Activation energy (E_a) was determined by plotting $\frac{1}{T_a}$ against $\ln(D_{eff})$, as shown in *Fig. 6;* then E_a was calculated using Eq. (11). E_a values for different air velocity levels, temperatures and IR radiations and related R^2 values are presented in *Table 4*. E_a values for food and agricultural materials were commonly located between 12.7 and 110 kJ/mol. Minimum and maximum values of E_a for terebinth were ranged between 44.41 and 59.13 kJ/mol, respectively. The maximum value of E_a was obtained for an air velocity of 1.76 m/s; for air velocities of 0.93 and 2.6 m/s, the activation energy decreased. Increasing the IR radiation power resulted in decreased activation energy. In terebinth fruits water is found as surface water and bounded water, most of the water being bounded; as a result water is transferred in the falling rate period, requiring a relatively high energy. Undesirable change of terebinth fruit such as color degradation in this drying condition is notable. Appropriate selection of air velocity and temperature would result in minimizing the quality damage. Activation energy of terebinth fruit (minimum value of 44.41 kJ/mol and maximum value of 59.13 kJ/mol) is relatively high, compared with the other agricultural products; the average value of E_a for tomato is 22.23 kJ/mol (Ruiz Celma *et al*., 2009a) and 41.41 kJ/mol for castor oil fruits (Perea-Flores *et al*., 2012).

Rupture force and energy. The required force and energy to create rupture of the terebinth fruit are presented in *Table 5*. It was noticed that the minimum force and energy to create rupture increased with increasing air temperature (from 40 to 70°C), air velocity (from 0.93 to 2.6 m/s) and IR radiation power (from 500 to 1500 W). Statistical analysis showed that the input parameters of air temperatures, IR radiation and air velocity have significant effects on the rupture force and energy ($P< 0.05$); the highest rupture force and energy for terebinth fruits were obtained for an air velocity of 2.6 m/s, an air temperature of 70°C and IR radiation power of 1500 W, while the lowest values of rupture force and energy were recorded for an air velocity of 0.93 m/s, an air temperature of 40°C and an IR radiation power of 500 W. The small rupturing forces and energies at low temperature might have resulted from the fact that the terebinth fruit preserves its soft texture at low temperatures, whereas higher temperature causes the hardening of the fruit. The proposed models for rupture force and energy models are as follows:

$$F_r = 17.33v + 1.291T_c + 0.0297w - 0.1189vT_c - 0.0028T_c w - 0.0002vw \qquad R^2 = 0.9536 \quad (14)$$

$$E_r = 294.8v + 16.07T_c + 0.6974w + 0.0051vT_c w - 2.624vT_c - 0.2665vw - 0.0111T_c w \qquad R^2 = 0.9700 \quad (15)$$

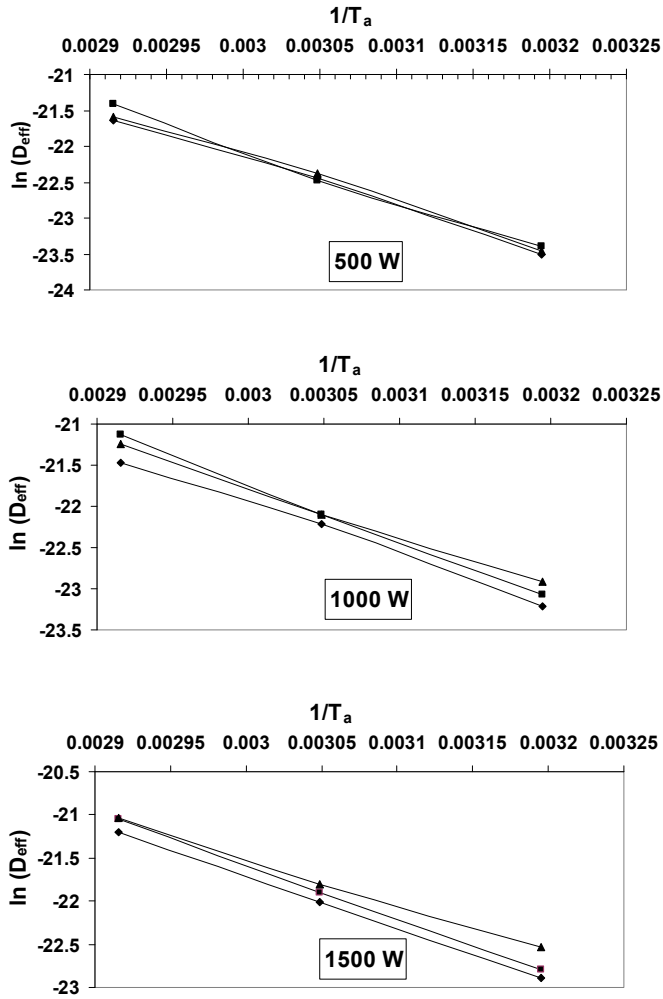

Figure 6 - ln(D_{eff}) against 1/T_a at different bed conditions (♦ 0.93 m/s, ■ 1.76 m/s and ▲2.6 m/s) for thin layer drying of terebinth seed

Table 5 - Effect of air temperature on rupture force and energy of terebinth seed

Temperature (°C)-IR radiation (W)	Fix bed (0.93 m/s)		Semi fluid bed (1.76 m/s)		Fluid bed (2.6 m/s)	
	Force (N)	Energy (N.mm)	Force (N)	Energy (N.mm)	Force (N)	Energy (N.mm)
40-500	72.4	896.2	76.7	1049.7	90.7	1140.7
55-500	89.3	1117.7	99.3	1226.8	103.7	1357.5
70-500	89.1	1180.4	108.7	1346.3	110.7	1478
40-1000	80.6	1028.6	88.7	1134.4	92.3	1210.2
55-1000	92.5	1157.8	103.7	1296.7	106.4	1422.6
70-1000	104.6	1203.6	112.8	1397.4	114	1555.8
40-1500	85.9	1054.7	96	1208.3	96.7	1251.6
55-1500	94.2	1168	105.1	1324	108.7	1454.6
70-1500	107	1219.8	114.6	1447.8	118.4	1619

CONCLUSIONS

Terebinth fruit drying behavior in a laboratory infrared dryer with air drying temperatures of 40, 55, 70°C, air velocity of 0.93, 1.76, 2.6 m/s and IR radiation power of 500, 1000, 1500 W were studied. Drying air temperature, air velocity and IR radiation power were important factors affecting the drying time.

The results showed that the best model for predicting drying kinetic was the Demir *et al*.

The effective moisture diffusivity, activation energy, specific energy consumption and shrinkage of terebinth fruit were evaluated.

The effective moisture diffusivity values ranged from 6.2×10^{11} to 7.3×10^{-10} m^2/s.

The highest effective moisture diffusivity was attained at an air velocity of 2.6 m/s, temperature of 70°C and IR radiation power of 1500 W.

The activation energy (E_a) values ranged from 44.4 to 59.13 kJ/mol.

The rupture force values ranged from 72.4 to 118.4 N and rupture energy values ranged from 896.2 to 1619 N mm.

The highest force and energy was obtained for terebinth fruit at air velocity of 2.6 m/s, temperature of 70°C and IR radiation of 1500 W.

REFERENCES

Abbasi Souraki B., Mowla D., 2008 - Axial and radial moisture diffusivity in cylindrical fresh green beans in a fluidized bed dryer with energy carrier: modeling with and without shrinkage. Journal of Food Engineering, 88, 9-19.

Altuntas E., Yildiz M., 2007 - Effect of moisture content on some physical and mechanical properties of faba bean (*Vicia faba* L.) grains. Journal of Food Engineering, 78, 174-183.

Altuntas E., Gercekcioglu R., Kaya, C., 2010 - Selected mechanical and geometric properties of different almond cultivars. International Journal Food Prop., 13(2), 282-293.

Amiri Chayjan R., Kaveh M., 2013 - Physical parameters and kinetic modeling of fix and fluid bed drying of terebinth seeds. Journal Food Processing and Preservation. doi:10.1111/jfpp.12092 (in press).

Amiri Chayjan R., Amiri Parian J., Esna-Ashari M., 2011 - Modeling of moisture diffusivity, activation energy and specific energy consumption of high moisture corn in a fixed and fluidized bed convective dryer. Spanish Journal of Agricultural Research, 9(1), 28-40.

Babalis S. J., Belessiotis V. G., 2004 - Influence of drying conditions on the drying constants and moisture diffusivity during the thin-layer drying of figs. Journal of Food Engineering, 65, 449-458.

Basman A., Yalcin S., 2011 - Quick-boiling noodle production by using infrared drying. Journal of Food Engineering, 106, 245-252.

Boudhrioua N., Bahloul N., Slimen I. B., Kechaou N., 2009 - Comparison on the total phenol contents and the color of fresh and infrared dried olive leaves. Industrial crops and products, 29, 412-419.

Bozkir O., 2006 - Thin-layer drying and mathematical modelling for washed dry apricots. Journal of Food Engineering, 77(1), 146-151.

Çağlar A., Toğrul I.T., Toğrul H., 2009 - Moisture and thermal diffusivity of seedless grape under infrared drying. Food and Bioproducts Processing, 87, 292-300.

Das I., Das S.K., Bal S., 2009 - Drying kinetics of high moisture paddy undergoing vibration-assisted infrared (IR) drying. Journal of Food Engineering, 95, 166-171.

Demir V., Gunhan T., Yagcioglu A.K., 2007 - Mathematical modeling of convection drying of green table olives. Biosystems Engineering, 98, 47-53.

Dondee S., Meeso N., Soponronnarit S., Siriamornpun S., 2011 - Reducing cracking and breakage of soybean grains under combined near-infrared radiation and fluidized-bed drying. Journal of Food Engineering, 104, 6-13.

Doymaz I., 2004a - Drying kinetics of white mulberry. Journal of Food Engineering, 61, 341-346.

Doymaz I., 2005 - Influence of pretreatment solution on the drying of sour cherry. Journal of Food Engineering, 78, 591-596.

Doymaz I., Ismail O., 2011- Drying characteristics of sweet Cherry. Food bioprod. process, 89, 31-38.

Duc L.A., Han J.W., Keum D.H., 2011 - Thin layer drying characteristics of rapeseed (*Brassica napus* L.). J. Stored Products Res., 47, 32-38.

Gharibzahedi S.M.T., Etemad V., Mirarab-Razi J., Foshat M., 2010 - Study on some engineering attributes of pine nut (*Pinus pinea*) to the design of processing equipment. Research in Agricultural Engineering, 56(3),99-106.

Gharibzahedi S.M.T., Mousavi S.M., Hamedi M., Khodaiyan M., 2012 - Comparative analysis of new Persian walnut cultivars: nut/kernel geometrical, gravimetrical, frictional and mechanical attributes and kernel chemical composition. Scientia Horticulturae, 135, 202-209.

Kaveh M., Amiri Chayjan R., 2014 - Predication of some physical and drying properties of terebinth seed (*Pistacia atlantica* L.) using artificial neural networks. Acta Scientiarum Polonorum Technologia Alimentaria, 13(1), 65-78.

Khir R., Pan Z., Salim A., Hartsough B.R., Mohamed S., 2011 - Moisture diffusivity of rough rice under infrared radiation drying. LW T - Food Science and Technology, 44, 1126-1132.

Manuwa S.I., Muhammad H.A., 2011 - Effects of moisture content and compression axis on mechanical properties of shea kernel. Journal of Food Engineering, 105, 144-148.

Niamnuy C., Nachaisin M., Poomsa-ad N., Devahastin S., 2012 - Kinetic modelling of drying and conversion/degradation of Iioflavones during infrared drying of soybean. Food Chemistry, 133, 946-952.

Pan Z., Shih C., McHugh T.H., Hirschberg E., 2008 - Study of banana dehydration using sequential infrared radiation heating and freeze-drying. LWT - Food Science and Technology, 41, 1944-1951.

Pathare P.B., Sharma G.P., 2006 - Effective moisture diffusivity of onion slices undergoing infrared convective drying. Biosystems Engineering, 93(3), 285–291.

Perea-Flores M.J., Garibay-Febles V., Chanona-Pérez J.J., Calderón-Domínguez G., Méndez-Méndez J.V., Palacios-González E., Gutiérrez-López G.F., 2012 - Mathematical modelling of castor oil seeds (*Ricinus communis*) drying kinetics in fluidized bed at high temperatures. Industrial Crops and Products, 38, 64-71.

Ponkham K., Meeso N., Soponronnarit S., Siriamornpun S., 2011 - Modeling of combined far-infrared radiation and air drying of a ring shaped-pineapple with/without shrinkage. Food and Bioproducts Processing, 90, 155–164.

Ruiz Celma A., Cuadros F., López-Rodríguez F., 2009a - Characterisation of industrial tomato by-products from infrared drying process. Food and Bioproducts Processing, 87, 282-291.

Ruiz Celma A., López-Rodríguez F., Cuadros Blázquez F., 2009b - Experimental modelling of infrared drying of industrial grape by-products. Food and Bioproducts Processing, 87, 247-253.

Sacilik K., Elicin A.K., Unal G., 2006 - Drying kinetics of Uryani plum in a convective hot-air dryer. Journal of Food Engineering, 76, 362–368.

Shi J., Pan Z., McHugh T.H., Wood D., Hirschberg E., Olson D., 2008 - Drying and quality characteristics of fresh and sugar-infused blueberries dried with infrared radiation heating. LWT - Food Science and Technology, 41, 1962-1972.

Toğrul I.T., Pehlivan D., 2004 - Modelling of drying kinetics of some fruits under open-air sun drying process. Journal of Food Engineering, 65, 413-425.

Wang J., Sheng K., 2006 - Far-infrared and microwave drying of peach. Food Science and Technology, 39(3), 247-255.

Zhu Y., Pan Z., McHugh T.H., Barrett D.M., 2010 - Processing and quality characteristics of apple slices processed under simultaneous infrared dry-blanching and dehydration with intermittent heating. Journal of Food Engineering, 97, 8-16.